

PARAMETERS OF A WATER-VORTEX STABILIZED ELECTRIC ARC CALCULATED BY USING DIFFERENT RADIATION MODELS

J. JENIŠTA

*Institute of Plasma Physics, Czech Acad. Sci., Za Slovankou 3, P. O. Box 17,
182 21 Praha 8, Czech Republic*

Received 4 April 2000;
final version 31 May 2000

The paper deals with a numerical modeling of parameters of a water-vortex stabilized electric arc in the case when re-absorption of plasma radiation is taken into consideration. The radiation losses from the arc are involved through the net emission coefficient which is, in this model, composed of two parts: the first term accounts for the net emission radiation loss inside the arc while the second term mostly represents re-absorption of radiation at the colder arc boundary. It was proved that re-absorption of radiation influences arc parameters in a specific manner. The calculated characteristics are in reasonable agreement with experiments made on the water plasma torch operating at the Institute.

1 Introduction

Water plasma torches with vortex stabilization produce oxygen-hydrogen plasma jet with unique physical and chemical properties. The rotation of water, created in the cylindrical chamber, is important for the stability of the shape of the vortex as well as for an electric arc to be ignited in the centre of this water vortex. A certain amount of the Joule input power within the arc column is dissipated in the vortex and causes evaporation of water. Further heating and ionization of the steam are the principal processes producing water plasma. The continuous inflow and heating create an overpressure in the discharge chamber, i.e. plasma is accelerated towards the outlet nozzle exit with extremely high flow velocity and enthalpy.

The arc with water-vortex stabilization has been commonly used for plasma spraying, however, it has been also successfully utilized in plasma cutting. Further, waste treatment and chemical vapour deposition seem to be the future perspective applications.

The computer results presented here refer to thermal, fluid dynamic and electrical characteristics of the water-plasma arc for the currents 300 and 400 A. Section 2 provides information about the model assumptions, numerical approach and boundary conditions, Sec. 3 shows the most important findings.

2 Description of the physical model

2.1 Assumptions and the set of equations

The two-dimensional axisymmetric numerical model includes the area between the cathode and the outlet nozzle of the arc discharge chamber. It is assumed that

the plasma flow is steady, laminar, mildly compressible and the plasma itself is in the state of local thermodynamic equilibrium. The production of water plasma, i.e. the rate of evaporation of a water wall, is in this model taken either from experiments or is calculated from radial conduction and radiation heat fluxes near the water-vapour transition [1, 2]. The complete set of conservation equations including the mass, electric charge, momentum and energy transport with temperature-dependent transport and thermodynamic properties is solved numerically by the control volume method [3]. The governing equations can be written in the vector notation as follows:

continuity equation:

$$\frac{\partial}{\partial t} \rho + \nabla \cdot (\rho \vec{u}) = 0 , \quad (1)$$

momentum equation:

$$\frac{\partial}{\partial t} (\rho \vec{u}) + \nabla \cdot (\rho \vec{u} \vec{u}) = -\nabla p + \nabla \cdot (\vec{j} \times \vec{B}) , \quad \tau_{ij} = \eta \left(\frac{\partial u_i}{\partial x_j} + \frac{\partial u_j}{\partial x_i} - \frac{2}{3} \delta_{ij} \frac{\partial u_l}{\partial x_l} \right) , \quad (2)$$

energy equation:

$$\frac{\partial}{\partial t} (\rho c_p T) + \nabla \cdot (\rho \vec{u} c_p T) - \frac{\partial p}{\partial t} = -\nabla \cdot (\lambda \nabla T) + \vec{j} \vec{E} + \vec{u} \nabla p + \frac{5}{2} \frac{k}{e} (\vec{j} \cdot \nabla T) - U_{net} , \quad (3)$$

charge continuity equation:

$$\nabla \cdot (\sigma \nabla \Phi) = 0 , \quad (4)$$

where \vec{u} is the velocity vector, p is the pressure, T is the temperature, \vec{j} is the current density. \vec{E} is the electric field strength, Φ is the electric potential, \vec{B} is the self-generated magnetic field, k is the Boltzmann constant and e is the elementary charge of electron.

The radiation losses from the arc are calculated through the net emission coefficient U_{net} in two ways:

$$U_{net} = k_1 U_e (T, 0) - k_2 f_a (\Theta) , \quad (5)$$

$$U_{net} = k_1 [U_e (T, 0) - \bar{U}_e (T, 0) \cdot (T_{wall}/T)^\gamma] . \quad (6)$$

The first terms on the right-hand sides of (5, 6) account for the net emission radiation loss inside the arc while the second terms represent re-absorption of radiation at the colder arc boundary (by means of the automodeling functions for absorption $f_a (\Theta)$ and $(T_{wall}/T)^\gamma$). $U_e (T, 0)$ is the emission coefficient for optically thin plasma, $\bar{U}_e (T, 0)$ is the mean value of $U_e (T, 0)$ over the elementary volume of plasma, k_1 and k_2 are constants for a given temperature profile, T_{wall} is the temperature of the cold plasma boundary. It is assumed in Eq. (5) (*model 1*) that re-absorption is proportional to $1/T$. For the details about this approach see [4]. Eq. (6) (*model 2*) assumes that re-absorption depends on temperature as $(1/T)^\gamma$, $\gamma \geq 0$, and it removes the additional assumption introduced in model 1 about the abrupt increase of the amount of re-absorbed radiation at the transition between the hot and cold plasma regions. The parameter γ is found in the calculations iteratively and its value depends on the amount of re-absorbed radiation.

2.2 Boundary conditions

The calculation region and the corresponding boundary conditions are shown in Fig. 1. Here u and v are the axial and radial components of the velocity. The dimensions are respectively $R = 3.3$ mm and $L = 65$ mm for the radius and the length. Along the cathode surface AB we assume no slip conditions for velocities, the temperature profile and the electric field strength are assigned to give the prescribed current intensity. The symmetry conditions are specified at the axis BC. The outlet velocity at CD is determined from the conservation of the total mass flow. Along the part of the DA line, the temperature of the outlet nozzle is kept at 473 K. The magnitude of the radial inflow velocity is derived from the specified mass flow rate.

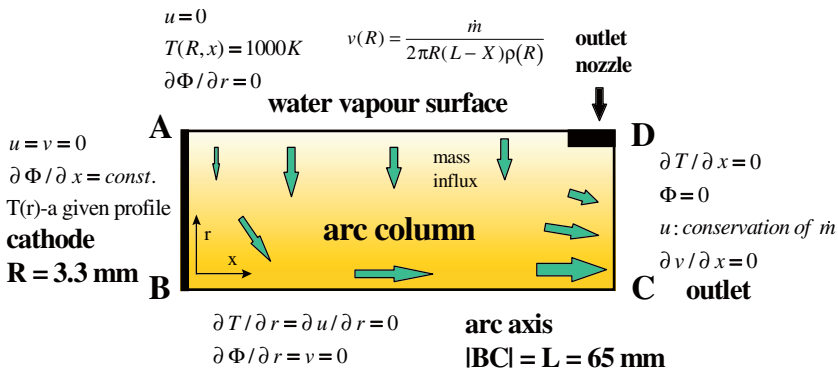


Fig. 1. Discharge area geometry. Dimensions of the outlet nozzle are $X = 5$ mm (axial direction) and 0.3 mm (radial direction).

3 Results and conclusions

Calculations carried out for the current intensities 300 A (mass flow rate $\dot{m} = 0.265$ g/s) and 400 A ($\dot{m} = 0.317$ g/s) for the models 1 and 2 showed the following dependencies for the fluid-dynamic, thermal and electric intensities: the higher is the amount of re-absorbed radiation, the lower (higher) are the outlet plasma velocities, temperatures and electric potential drops (current densities and electric field strengths). For the 400 A arc when 20 % of radiation is re-absorbed we obtain the outlet axial velocities (at the point C in Fig. 1) 4 200 m/s (4 500 m/s), temperatures 21 600 K (22 100 K), potential drops 165 V (165 V), current densities $3.71 \cdot 10^7$ A/m² ($3.64 \cdot 10^7$ A/m²) for the model 1 (model 2, $\gamma = 0.263$). Good agreement between the two radiation models is valid not only for the outlet axial values but also for the shapes of the corresponding profiles within the plasma discharge chamber. Radial profiles of the net emission coefficient U_{net} (Fig. 2) at the

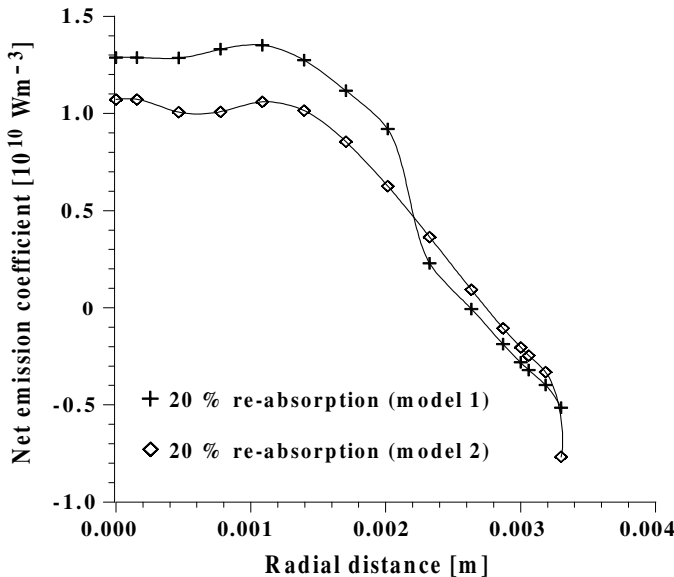


Fig. 2. Radial profiles of the net emission coefficient at the axial position ≈ 4.1 cm downstream from the cathode. $I = 400$ A, $\dot{m} = 0.317$ g/s.

position ≈ 4.1 cm downstream from the cathode show that axial values of U_{net} for the model 1 are higher and, more far from the axis, U_{net} decreases steeper than for the model 2. This is obvious because the assumption of the abrupt increase of the absorption automodeling function $f_a(\Theta)$ at the transition region between the hot and cold plasma regions is included in the model 1.

In conclusion we can say that the model 2 (Eq. (6)) simplifies the model 1 and represents a good alternative for use in numerical simulations where the net emission coefficient procedure is employed. Despite the fact that the corresponding absorption functions $f_a(\Theta)$ and $(T_{wall}/T)^\gamma$ give different values along the arc radius, both models provide comparable numerical results which are in satisfactory agreement with experimental data.

References

- [1] J. Jeništa: J. Appl. Phys. **32** (1999) 2763.
- [2] J. Jeništa: J. Appl. Phys. **32** (1999) 2777.
- [3] S.V. Patankar: *Numerical heat transfer and fluid flow*. McGraw-Hill, New York, 1980.
- [4] J. Jeništa: in *Proc. 14th Int. Symp. on Plasma Chemistry (ISPC)* (Ed. M. Hrabovský). Local Org. Committee of the 14th ISPC, Praha, 1999, Vol. I, p.281.